

# Dibenzophosphapentaphenes: Exploiting P Chemistry for Gap Fine-Tuning and Coordination-Driven Assembly of Planar Polycyclic Aromatic Hydrocarbons

Pierre-Antoine Bouit,<sup>†</sup> Aude Escande,<sup>†</sup> Rózsa Szűcs,<sup>‡</sup> Dénes Szieberth,<sup>‡</sup> Christophe Lescop,<sup>†</sup> László Nyulászi,<sup>‡</sup> Muriel Hissler,<sup>\*,†</sup> and Régis Réau<sup>\*,†</sup>

<sup>†</sup>Institut des Sciences Chimiques de Rennes, UMR 6226 CNRS - Université de Rennes 1, Campus de Beaulieu, 35042 Rennes Cedex, France

<sup>‡</sup>Department of Inorganic Chemistry, Budapest University of Technology and Economics, H-1521 Budapest, Hungary

## Supporting Information

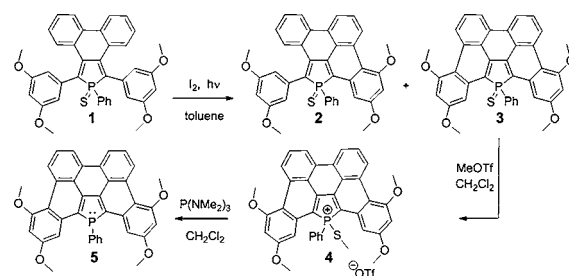
**ABSTRACT:** A synthetic route to planar P-modified polycyclic aromatic hydrocarbons (PAHs) is described. The presence of a reactive  $\sigma^3, \lambda^3$ -P moiety within the  $sp^2$ -carbon scaffold allows the preparation of a new family of PAHs displaying tunable optical and redox properties. Their frontier molecular orbitals (MOs) are derived from the corresponding phosphole MOs and show extended conjugation with the entire  $\pi$  framework. The coordination ability of the P center allows the coordination-driven assembly of two molecular PAHs onto a  $Au^I$  ion.

Polycyclic aromatic hydrocarbons (PAHs), such as benzocoronenes or nanographenes, are of great potential in molecular electronics for the development of efficient optoelectronic devices (solar cells, field-effect transistors, etc.).<sup>1</sup> The possibility of performing molecular engineering of PAHs using the power of organic chemistry is a key toward these applications. Indeed, HOMO–LUMO gap and supramolecular assembly of PAHs can be controlled through modification of the size of the  $\pi$ -conjugated system or/and by the proper choice of lateral aliphatic substituents.<sup>2</sup> An alternative appealing strategy involves the incorporation of heteroatoms (N,<sup>3</sup> O,<sup>4</sup> S,<sup>5</sup> B<sup>6</sup>) within the conjugated  $sp^2$ -carbon backbones of PAHs. Surprisingly, no fully planarized P-containing PAHs have been described to date,<sup>7</sup> although  $\sigma^3, \lambda^3$ -P derivatives have proven to be powerful platforms for molecular engineering of  $\pi$ -conjugated scaffolds. For example, both the HOMO–LUMO gap and supramolecular organization of phosphole-modified  $\pi$  systems can be readily controlled using the versatile reactivity (nucleophilicity, coordination ability) of the  $\sigma^3, \lambda^3$ -P centers.<sup>8</sup> Herein we report that this approach based on P chemistry can be extended to planar P-modified PAHs, with the synthesis of dibenzophosphapentaphenes. Of particular interest, exploiting the reactivity of the P center allows straightforward fine-tuning of the gap in this novel family of PAH derivatives. Furthermore, these compounds can be coordinated to metal ions, offering an unprecedented way of assembling PAHs using coordination chemistry.

The synthesis of P-containing PAHs using classical approaches (Scholl reaction, thermolysis, etc.)<sup>1a</sup> with pentaphenylphosphole derivatives failed because of the presence of

the reactive phosphorus heterocycle. Only photocyclization appeared to be a suitable synthetic method,<sup>9</sup> and the fused biphenyl[*b,d*]thioxophosphole **1**<sup>10</sup> (Scheme 1) was finally

## Scheme 1. Synthesis of $\sigma^3, \lambda^3$ -Dibenzophosphapentaphene 3



designed as a key precursor following numerous unsuccessful tries. For example, the choice of the P=S function was crucial, since this P moiety is less prone to react with in situ-generated protic acid than the corresponding P=O function.<sup>11</sup> Derivative **1** (<sup>31</sup>P NMR: +58.7 ppm) was obtained using the classic Fagan–Nugent heterole route<sup>12</sup> followed by sulfurization. Photocyclization of **1** over 20 h using the Katz-modified method<sup>13</sup> afforded a mixture of the monocyclized derivative **2** and the fully cyclized target dibenzophosphapentaphene **3** (Scheme 1). Increasing the reaction time did not improve the yield of **3**. Both compounds are air-stable and soluble in common organic solvents (THF, CH<sub>2</sub>Cl<sub>2</sub>) and were isolated in pure form (yields: **2**, 50%; **3**, 20%) after purification by chromatography. The two products were fully characterized by NMR spectroscopy and high-resolution mass spectrometry (HRMS). Their <sup>31</sup>P chemical shifts are typical for thioxophosphole derivatives (<sup>31</sup>P NMR: **2**, +51.6 ppm; **3**, +46.0 ppm), and the simplicity of the <sup>1</sup>H NMR spectrum of **3** is consistent with a highly symmetric skeleton [see the Supporting Information (SI)].

Definitive proof for the proposed structure was provided by an X-ray crystallographic study performed on single crystals of **3** (Figure 1). The  $sp^2$ -carbon framework is planar (maximum deviation from the mean  $sp^2$ -C plane, 0.15 Å), and the P atom

Received: January 6, 2012

Published: April 4, 2012

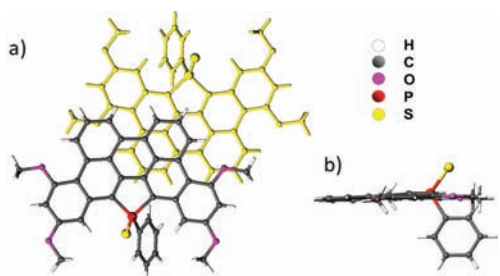


**Figure 1.** X-ray crystallographic structure of **3**: (a) view of the discrete dimers observed in the packing structure; (b) view of **3** perpendicular to the  $sp^2$ -C plane.

lies within the  $sp^2$ -C plane (Figure 1b). The C–C bond lengths range from 1.35 to 1.49 Å, as observed in prototype benzocoronene derivatives,<sup>14</sup> and the valence angles around the  $sp^2$ -C atoms vary from 114.3 to 125.5°. The  $\sigma^4, \lambda^5$ -phosphorus atom has a pyramidal shape (Figure 1b) with the usual valence angles, and the C–C and C–P bond lengths within the phosphole ring are classic.<sup>8a</sup> This solid-state structure shows that **3** combines the characteristic structural features of PAH and phosphole derivatives. In the solid state, **3** forms discrete head-to-tail  $\pi$  dimers (Figure 1a) with an intermolecular distance of 3.45 Å,<sup>15</sup> similar to that observed in other benzocoronenes or in graphite.<sup>14</sup>

Having constructed the P-modified PAH backbone, the next step was to desulfurize<sup>16</sup> the phosphole ring to obtain a functionalizable  $\sigma^3, \lambda^3$ -P-dibenzophosphapentaphene. Treatment of thioxophosphole **3** with methyl triflate afforded phospholium ion **4** (<sup>31</sup>P NMR: +50.1 ppm), which was isolated as a purple solid in 60% yield (Scheme 1). Derivative **4**, which is the first isolated phospholium ion bearing a P–S bond, is remarkably air- and moisture-stable in solution and in the solid state. The solid-state structure of this cationic dibenzophosphapentaphene (Figure S12 in the SI) is superimposable on that of its neutral precursor **3**, showing that chemical modifications of the P moiety do not alter the planar  $sp^2$ -carbon backbone. Phospholium **4** was then converted into its  $\sigma^3, \lambda^3$ -analogue **5** by treatment with the nucleophilic phosphane  $P(NMe_2)_3$  (Scheme 1).  $\sigma^3, \lambda^3$ -Dibenzophosphapentaphene **5** was isolated in 50% yield as an air-stable yellow powder that is moderately soluble in THF or  $CH_2Cl_2$ . Its <sup>31</sup>P NMR chemical shift (–2.9 ppm) is a usual value for phosphole derivatives,<sup>8a</sup> and the proposed structure is consistent with its NMR and MS data (see the SI).

The P center in compound **5** retains versatile reactivity, as illustrated by its transformations into oxidized phospholes (thioxophosphole **3**, oxophosphole **6**), phospholiums **4** and **7**, and neutral  $Au^I$  complex **8** in almost quantitative yields (Scheme 2). These compounds exhibit the expected multinuclear NMR and MS data (see the SI). Overall, a family of neutral and cationic dibenzophosphapentaphenes derivatives **3–8** was prepared (Scheme 2). This nicely illustrates that introducing a reactive  $\sigma^3, \lambda^3$ -P center within the PAH framework allows molecular engineering to be performed readily.

To evaluate the impact of the P modifications on the electronic properties of these PAHs, the optical and electrochemical properties of dibenzophosphapentaphenes **3–8** were investigated in  $CH_2Cl_2$ . The absorption spectrum of **5** consists of a large, structured band in the visible range ( $\lambda_{max} = 472$  nm; Table 1) that displays the typical PAH-like hyperfine structure (Figure 2a).<sup>1a</sup> Neutral  $\sigma^4$ -P derivatives **3**, **6**, and **8** (Scheme 2)

## Scheme 2. Chemical Derivatization of $\sigma^3, \lambda^3$ -Dibenzophosphapentaphene **5**

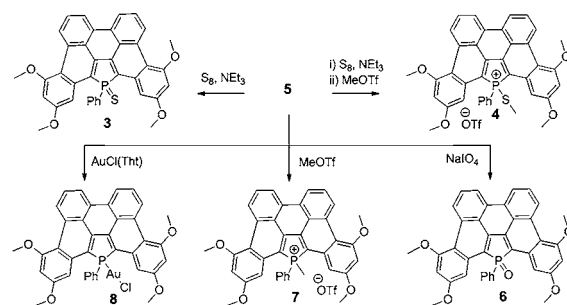


**Table 1.** Photophysical and Electrochemical Data

compd	absorption <sup>a</sup>		fluorescence <sup>a</sup>		redox potentials (V) <sup>c</sup>	
	$\lambda_{abs}$ (nm)	log $\epsilon$	$\lambda_{em}$ (nm)	$\phi_F$ <sup>b</sup>	$E_1^{ox}$	$E_1^{red}$
<b>3</b>	514	4.04	544	0.21	0.71	–1.70 <sup>d</sup>
<b>4</b>	569	3.95	669	0.03	1.01	–1.04
<b>5</b>	472	4.34	489	0.80	0.44	<–2.10
<b>6</b>	524	4.11	549	0.52	0.77	–1.71 <sup>d</sup>
<b>7</b>	554	4.00	599	0.19	0.97	–1.31 <sup>d</sup>
<b>8</b>	508	4.14	537	0.08	0.75	–1.67 <sup>d</sup>

<sup>a</sup>In  $CH_2Cl_2$  ( $10^{-5}$  M). <sup>b</sup>Measured relative to fluorescein (NaOH, 0.1 M),  $\phi_{ref} = 0.9$ . <sup>c</sup>Measured in  $CH_2Cl_2$  containing  $Bu_4N^+PF_6^-$  (0.2 M) at a scan rate of 100  $mV s^{-1}$ . Potentials in V vs ferrocene/ferrocenium. <sup>d</sup>Reversible process

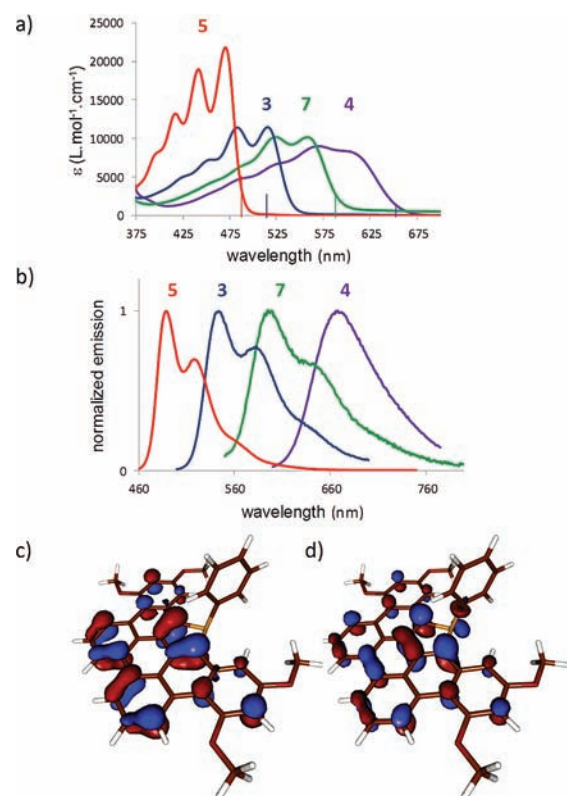


**Figure 2.** (a) UV-vis absorption and TD-DFT-simulated spectra (vertical lines). (b) Normalized emission spectra of **3** (blue), **4** (purple), **5** (red), and **7** (green) in  $CH_2Cl_2$  ( $10^{-5}$  M). (c, d) Kohn-Sham MOs of **5**: (c) HOMO; (d) LUMO.

exhibit red-shifted absorption spectra with similar shapes and absorption maxima (Table 1, Figure 2a). A larger bathochromic

shift is observed with P-alkyl and P-S phospholium salts **7** and **4** (Table 1). Remarkably, the absorption spectra of the dibenzophosphapentaphenes **3–8**, which have the same polycyclic aromatic C skeleton but different P moieties (Scheme 2), vary over a wide range covering almost the entire visible spectrum (Figure 2a). All of these dibenzophosphapentaphenes are fluorescent in solution, with a gradual red shift of  $\lambda_{em}$  in the series **5/3/7/4** (Table 1, Figure 2b). The Stokes shifts are reasonably small for these rigid structures (**5**,  $\Delta\bar{\nu} = 737 \text{ cm}^{-1}$ ; **3**,  $\Delta\bar{\nu} = 1072 \text{ cm}^{-1}$ ; **7**,  $\Delta\bar{\nu} = 1355 \text{ cm}^{-1}$ ) and the emission bands are structured, suggesting a small rearrangement of these molecules upon photoexcitation. Therefore, their quantum yields are relatively high (>20%; Table 1). In contrast, derivative **4** presents a larger Stokes shift ( $\Delta\bar{\nu} = 2875 \text{ cm}^{-1}$ ) accompanied by a decrease in the fluorescence quantum yield (3%).

Analysis of the cyclic voltammetry data showed that the chemical modifications performed on the P center of **5** lead to a gradual increase in the oxidation and reduction potentials in the series **5/3/7/4** (Table 1). The variation is even more pronounced for the reduction potential, revealing that phospholium salts **4** and **7** have rather high electron affinities. It is noteworthy that **3**, **6**, **7**, and **8** show reversible reduction waves, indicating sufficient stability in their reduced state under the measurement conditions (Table 1). The evolution of the redox potentials within the **5/3/7/4** series is consistent with the decrease in the optical gap (Figure 2a).

To gain more insight into the electronic properties of these novel P-modified PAHs, time-dependent density functional theory (TD-DFT) calculations at the B3LYP/6-31+G\* level of theory<sup>17</sup> were performed.<sup>18</sup> This theoretical study showed that the long-wavelength UV-vis absorption of PAHs **3–7** mainly results from the HOMO–LUMO transition.<sup>19</sup> These frontier molecular orbitals are similar throughout the series **5–7** (**5**, Figure 2c,d; **3–7**, Figure S14). These  $\pi$  MOs are highly delocalized on the  $sp^2$ -carbon skeletons with a significant contribution of the respective phosphole ring orbitals (Figure S15).<sup>20</sup> The HOMO, which has a nodal plane on the phosphorus atom, is influenced by the inductive effects of the P substituents. This explains why the shape of these orbitals is unaltered upon modification of the P moiety (Figure S14). The LUMO is subjected to the negative hyperconjugative interaction between the  $\sigma^*_{P\text{Substituent}}$  MO and the MOs of the  $sp^2$ -carbon framework. This results in stabilization of this empty level for  $\sigma^4$ -P-containing neutral and cationic systems and also increases the antiaromatic character of these heteroles.<sup>8b,21</sup> This influence of the P substituent can be nicely seen through the increasing weight of the P atom in the LUMO (Figure S14), especially for cationic systems **4** and **7**, which exhibit the highest reduction potentials (Table 1). It is interesting to note that the effect of P substitution on the electronic properties and frontier MOs of these P-modified PAHs follows the same trend as for the parent phosphole.<sup>20</sup> Overall, these experimental and theoretical data show that local chemical modification of the P moiety of dibenzophosphapentaphenes is a powerful means of fine-tuning the gap of these novel planar PAH derivatives.

The reactive P center in **5** also offers an unprecedented way of organizing PAHs using coordination chemistry, as illustrated by the assembly of two  $\sigma^3, \lambda^3$ -dibenzophosphapentaphenes **5** on a  $Au^I$  ion (Figure 3). Complex **8** (Scheme 2) was reacted with  $AgOTf^{22}$  and free ligand **5**, affording the new complex **9** ( $^{31}P$  NMR: +40.8 ppm). An X-ray crystallographic study confirmed the unique structure of complex **9**, in which two PAHs are

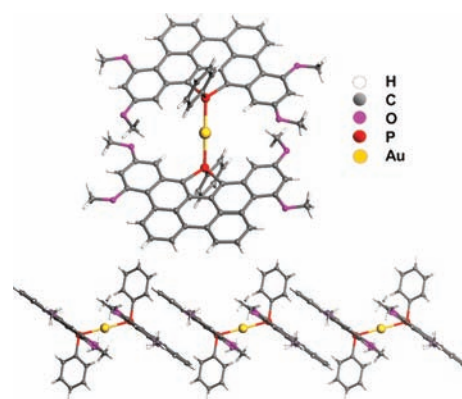


**Figure 3.** X-ray crystallographic structure of  $Au^I$ -complex **9** and a view of the infinite columns along the crystallographic *b* axis.

coordinated to the metal ion (Figure 3).<sup>23</sup> The P–Au–P fragment is linear (P–Au–P,  $180.0^\circ$ ), and the two highly planar  $sp^2$ -C skeletons of **5** exhibit an anti conformation with respect to the P–Au–P moiety (Figure 3). Interestingly, the packing of **9** is deeply modified relative to those of derivatives **3** and **4**. Intermolecular  $\pi$ – $\pi$  interactions between coordinated dibenzophosphapentaphenes take place ( $\pi$ – $\pi$  distances, 3.50 Å), affording infinite columns of  $\pi$ -stacked complexes **9** (Figure 3).<sup>15</sup> In view of the rich coordination chemistry of phosphole derivatives,<sup>8a</sup> the fact that **5** behaves as a classic two-electron P donor toward metal centers opens an avenue for coordination-driven assembly of phosphorus-modified PAHs.

In conclusion, a synthetic route to the first planar  $\sigma^3, \lambda^3$ -P-modified PAH is described. The presence of a reactive P moiety within the  $sp^2$ -C skeleton allows the facile synthesis of a new family of PAHs with tunable optical and electrochemical properties using a single precursor. This molecular engineering of PAHs based on P chemistry and their assembly using coordination chemistry shows the potential of modifying planar  $\pi$ -extended frameworks using organophosphorus fragments.

## ■ ASSOCIATED CONTENT

### 📄 Supporting Information

Experimental procedures; NMR data; X-ray crystallographic data and CIF files for **3**, **4**, and **9**; computational procedures and data; and HOMO and LUMO plots and energies for **3–7** and the related 1-methylphospholes. This material is available free of charge via the Internet at <http://pubs.acs.org>.

## ■ AUTHOR INFORMATION

### ✉ Corresponding Author

[muriel.hissler@univ-rennes1.fr](mailto:muriel.hissler@univ-rennes1.fr); [regis.reau@univ-rennes1.fr](mailto:regis.reau@univ-rennes1.fr)

### Notes

The authors declare no competing financial interest.

## ■ ACKNOWLEDGMENTS

This work was supported by the Ministère de la Recherche et de l'Enseignement Supérieur, the Centre National de la Recherche Scientifique (CNRS), the Institut Universitaire de France (IUF), and the Région Bretagne. COST CM0802 (Phoscinet) and TAMOP-4.2.2/B-10/1-2010-0009 are also acknowledged.

## REFERENCES

- (1) (a) Watson, M. D.; Fechtenkotter, A.; Müllen, K. *Chem. Rev.* **2001**, *101*, 1267. (b) Wu, J. S.; Pisula, W.; Müllen, K. *Chem. Rev.* **2007**, *107*, 718. (c) Schmidt-Mende, L.; Fechtenkötter, A.; Müllen, K.; Moons, E.; Friend, R. H.; MacKenzie, J. D. *Science* **2001**, *293*, 1119. (d) Pisula, W.; Feng, X.; Müllen, K. *Chem. Mater.* **2011**, *23*, 554.
- (2) (a) Pisula, W.; Feng, X.; Müllen, K. *Adv. Mater.* **2010**, *22*, 3634. (b) Yan, X.; Li, L.-S. *J. Mater. Chem.* **2011**, *21*, 3295.
- (3) (a) Draper, S. M.; Gregg, D. J.; Madathil, R. *J. Am. Chem. Soc.* **2002**, *124*, 3486. (b) Draper, S. M.; Gregg, D. J.; Schofield, E. R.; Browne, W. R.; Duati, M.; Vos, J. G.; Passaniti, P. *J. Am. Chem. Soc.* **2004**, *126*, 8694. (c) Wu, D. Q.; Pisula, W.; Enkelmann, V.; Feng, X. L.; Müllen, K. *J. Am. Chem. Soc.* **2009**, *131*, 9620. (d) Davis, N. K. S.; Thompson, A. L.; Anderson, H. L. *J. Am. Chem. Soc.* **2011**, *133*, 30. (e) Fogel, Y.; Kastler, M.; Wang, Z.; Andrienko, D.; Bodwell, G. J.; Müllen, K. *J. Am. Chem. Soc.* **2007**, *129*, 11743. (f) Wu, D.; Pisula, W.; Enkelmann, V.; Feng, X.; Müllen, K. *J. Am. Chem. Soc.* **2009**, *131*, 9620. (g) Wu, D. Q.; Feng, X. L.; Takase, M.; Haberecht, M. C.; Müllen, K. *Tetrahedron* **2008**, *64*, 11379. (h) Gregg, D. J.; Fitchett, C. M.; Draper, S. M. *Chem. Commun.* **2006**, 3090.
- (4) Wu, D.; Pisula, W.; Haberecht, M. C.; Feng, X.; Müllen, K. *Org. Lett.* **2009**, *11*, 5686.
- (5) (a) Martin, C. J.; Gil, B.; Perera, S. D.; Draper, S. M. *Chem. Commun.* **2011**, 47, 3616. (b) Feng, X.; Wu, J.; Ai, M.; Pisula, W.; Zhi, L.; Rabe, J. P.; Müllen, K. *Angew. Chem., Int. Ed.* **2007**, *46*, 3033. (c) Gorodetsky, A. A.; Chiu, C.-Y.; Schiros, T.; Palma, M.; Cox, M.; Jia, Z.; Sattler, W.; Kymissis, I.; Steigerwald, M.; Nuckolls, C. *Angew. Chem., Int. Ed.* **2010**, *49*, 7909. (d) Benschafut, R.; Rabinovitz, M.; Hoffman, R. E.; Ben-Mergui, N.; Müllen, K.; Iyer, V. S. *Eur. J. Org. Chem.* **1999**, 37.
- (6) (a) Hatakeyama, T.; Hashimoto, S.; Seki, S.; Nakamura, M. *J. Am. Chem. Soc.* **2011**, *133*, 18614. (b) Zhou, Z.; Wakamiya, A.; Kushida, T.; Yamaguchi, S. *J. Am. Chem. Soc.* **2012**, *134*, 4529.
- (7) A curved  $\pi$ -extended triarylphosphine was recently described. See: Hatakeyama, T.; Hashimoto, S.; Nakamura, M. *Org. Lett.* **2011**, *13*, 2130.
- (8) (a) Baumgartner, T.; Réau, R. *Chem. Rev.* **2006**, *106*, 4681. (b) Matano, Y.; Saito, A.; Fukushima, T.; Tokudome, Y.; Suzuki, F.; Sakamaki, D.; Kaji, H.; Ito, A.; Tanaka, K.; Imahori, H. *Angew. Chem., Int. Ed.* **2011**, *50*, 8016. (c) Bruch, A.; Fukazawa, A.; Yamaguchi, E.; Yamaguchi, S.; Studer, A. *Angew. Chem., Int. Ed.* **2011**, *50*, 12094. (d) Ren, Y.; Kan, W. H.; Henderson, M. A.; Bomben, P. G.; Berlinguette, C. P.; Thangadurai, V.; Baumgartner, T. *J. Am. Chem. Soc.* **2011**, *133*, 17014. (e) Graule, S.; Rudolph, M.; Vanthuyne, N.; Autschbach, J.; Roussel, C.; Crassous, J.; Réau, R. *J. Am. Chem. Soc.* **2009**, *131*, 3183. (f) Nohra, B.; Graule, S.; Lescop, C.; Réau, R. *J. Am. Chem. Soc.* **2006**, *128*, 3520. (g) Chen, H.; Delaunay, W.; Yu, L.; Joly, D.; Wang, Z.; Li, J.; Wang, Z.; Lescop, C.; Tondelier, D.; Geffroy, B.; Duan, Z.; Hissler, M.; Mathey, F.; Réau, R. *Angew. Chem., Int. Ed.* **2012**, *51*, 214. (h) Benkő, Z.; Nyulászai, L. *Top. Heterocycl. Chem.* **2009**, *19*, 27.
- (9) Fadhel, O.; Szieberth, D.; Deborde, V.; Lescop, C.; Nyulászai, L.; Hissler, M.; Réau, R. *Chem.—Eur. J.* **2009**, *15*, 4914.
- (10) Related bithienyl[*b,d*]phospholes were recently described. See: Matano, Y.; Miyajima, T.; Fukushima, T.; Kaji, H.; Kimura, Y.; Imahori, H. *Chem.—Eur. J.* **2008**, *14*, 8102.
- (11) Protonation of the strongly polarized P=O function is the first step towards decomposition of the phosphole ring.
- (12) Fagan, P. J.; Nugent, W. A. *J. Am. Chem. Soc.* **1988**, *110*, 2310.
- (13) Liu, L.; Yang, B.; Katz, T. J.; Poindexter, M. K. *J. Org. Chem.* **1991**, *56*, 3769.
- (14) Herwig, P. T.; Enkelmann, V.; Schmelz, O.; Müllen, K. *Chem.—Eur. J.* **2000**, *6*, 1834.
- (15) The  $\pi$ - $\pi$  distances were obtained by measuring the distances between the mean planes (including all of the C and P atoms of the planar scaffold) of two neighboring molecules.
- (16) Omelańczuk, J.; Mikołgajczyk, M. *Tetrahedron Lett.* **1984**, *25*, 2493.
- (17) A systematic study showed that TD-DFT with the B3LYP functional provides good results for vertical excitation energies of organic molecules. See: Jacquemin, D.; Wathelet, V.; Perpète, E. A.; Adamo, C. *J. Chem. Theory Comput.* **2009**, *9*, 2420.
- (18) DFT calculations were performed using the Gaussian 03 suite of programs. See: Frisch, M. J.; Trucks, G. W.; Schlegel, H. B.; Scuseria, G. E.; Robb, M. A.; Cheeseman, J. R.; Montgomery, J. A., Jr.; Vreven, T.; Kudin, K. N.; Burant, J. C.; Millam, J. M.; Iyengar, S. S.; Tomasi, J.; Barone, V.; Mennucci, B.; Cossi, M.; Scalmani, G.; Rega, N.; Petersson, G. A.; Nakatsuji, H.; Hada, M.; Ehara, M.; Toyota, K.; Fukuda, R.; Hasegawa, J.; Ishida, M.; Nakajima, T.; Honda, Y.; Kitao, O.; Nakai, H.; Klene, M.; Li, X.; Knox, J. E.; Hratchian, H. P.; Cross, J. B.; Bakken, V.; Adamo, C.; Jaramillo, J.; Gomperts, R.; Stratmann, R. E.; Yazyev, O.; Austin, A. J.; Cammi, R.; Pomelli, C.; Ochterski, J. W.; Ayala, P. Y.; Morokuma, K.; Voth, G. A.; Salvador, P.; Dannenberg, J. J.; Zakrzewski, V. G.; Dapprich, S.; Daniels, A. D.; Strain, M. C.; Farkas, O.; Malick, D. K.; Rabuck, A. D.; Raghavachari, K.; Foresman, J. B.; Ortiz, J. V.; Cui, Q.; Baboul, A. G.; Clifford, S.; Cioslowski, J.; Stefanov, B. B.; Liu, G.; Liashenko, A.; Piskorz, P.; Komaromi, I.; Martin, R. L.; Fox, D. J.; Keith, T.; Al-Laham, M. A.; Peng, C. Y.; Nanayakkara, A.; Challacombe, M.; Gill, P. M. W.; Johnson, B.; Chen, W.; Wong, M. W.; Gonzalez, C.; Pople, J. A. *Gaussian 03*, revision C.02; Gaussian, Inc.: Wallingford CT, 2004. The MOs were visualized using the MOLDEEN program. See: Schaftenaar, G.; Noordik, J. H. *J. Comput.-Aided Mol. Des.* **2000**, *14*, 123–134. More details concerning the calculations are given in the SI.
- (19) The contribution of the HOMO–LUMO excitation was 0.65 for all of the molecules investigated; the coefficients for other electron configurations were smaller than 0.12.
- (20) Hay, C.; Hissler, M.; Fischmeister, C.; Rault-Berthelot, J.; Toupet, L.; Nyulászai, L.; Réau, R. *Chem.—Eur. J.* **2001**, *7*, 4222.
- (21) Nyulászai, L.; Hollóczki, O.; Lescop, C.; Hissler, M.; Réau, R. *Org. Biomol. Chem.* **2006**, *4*, 996.
- (22) Escallé, A.; Mora, G.; Gagosz, F.; Mézailles, N.; Le Goff, X. F.; Jean, Y.; Le Floch, P. *Inorg. Chem.* **2009**, *48*, 8415.
- (23) A “squeeze” treatment was necessary to remove the scattering contribution of highly disordered CH<sub>2</sub>Cl<sub>2</sub> molecules and CF<sub>3</sub>SO<sub>3</sub><sup>-</sup> counterions that could not be satisfactory modeled (see the SI).